JOURNAL OF THE KOREAN ASTRONOMICAL SOCIETY
27: 147 ~ 158, 1994

A HIGHLY DISTURBED MOLECULAR CLOUD S287: I. CO OBSERVATIONS AND KINEMATICS

LEE, YOUNGUNG
Korea Astronomy Observatory, Taejon, Korea
(Received Sep. 23, 1994; Accepted Oct. 17, 1994)

ABSTRACT

We have obtained high angular resolution maps toward a molecular cloud associated with an HII region S287 and studied mainly kinematics of the cloud. The mapped region is 1.5 square degrees of the cloud in the transitions of ^{12}CO and ^{13}CO $J = 1 - 0$. We have obtained a large range of mass, 1.3×10^4 $M_\odot$,to 7.2×10^4 $M_\odot$ using three different techniques. The S287 molecular cloud shows a very disturbed feature: velocity field of the cloud is very complicated, and shows several arcs. It is likely that the southern part of cloud is being disrupted by the residing HII region S287 as well as external perturbing sources. In addition to an HII region, five bipolar outflows are also disturbing the molecular gas significantly. The large virial mass and the very disturbed morphology may reflect the fact that the cloud is not gravitationally bound system, as in the case of nearby giant molecular cloud (GMC) G216-2.5. The several arc structure and the filamentary features are possibly driven by external strong stellar winds, and these external perturbing sources may be driving the second generation of star-forming activities on the edges of the S287 molecular cloud.

I. INTRODUCTION

Giant molecular clouds (GMCs) in our Galaxy are a major component of interstellar medium, and also major star forming sites. Thus, the fundamental goal of GMCs' study is to understand how they evolve from more diffuse interstellar medium and how they start to form stars. In fact, GMCs are usually associated with active star forming activities with a few exceptional cases (Lee, Snell and Dickman 1994), and they are providing the initial conditions for the process of active star formation. Investigation of GMCs has been focused both on individual (Blitz 1991 and references therein) and statistical studies (Scoville *et al.* 1987; Solomon *et al.* 1987; Lee, Snell, and Dickman 1990). Also there have been several studies on selected large areas, which are usually complicated regions (Carpenter 1994; Lee 1992).

S287 HII region and associated molecular cloud (hereafter, we call it simply S287, or S287 molecular cloud) is listed in Lynds Dark Nebulae Catalog (Lynds 1962) as L1650, and also listed in Lynds Bright Nebulae Catalog (Lynds 1965) as LBN 1012. At the position of l=217°.73, b=−0°.69 there is an open cluster, which is also named as NGC 2311. The V_{LSR} of the molecular cloud (+27 km s^{-1})is almost the same as that of G216-2.5. Recently, Lee *et al.* (1994) have claimed that the G216-2.5 is a remnant cloud from a past episode of massive star formation, and the progenitor star-forming complex may have included S287 molecular cloud. S287 (l = 218°.1, b=−0°.4), is located ~ 100pc from a cold, massive GMC G216-2.5, and shows a quite different feature from G216-2.5: it has very active star forming activities and its morphology seems to be very disturbed. Iwata *et al.* (1989; unpublished) reported that there are five bipolar outflows residing in S287 molecular cloud (Fukui 1989). Located toward the concentration of gas at l = 217°.4 and b =−0°.1 is the bipolar nebula NS14. Neckel *et al.* (1989) found four stars of spectral type B0.5 to A5 associated with this bipolar nebula that are deeply embedded within the dense molecular cloud. Thus, unlike G216-2.5, there are several sites of massive star formation within this cloud. However, S287 has never been a main subject for GMC study except partial study (Lee *et al.* 1994), though it has many peculiar features. More detailed and high resolution study on this object is required to discuss the disturbed morphology and velocity field,

and star forming activities. To further address these issues we have obtained high angular resolution maps of S287 molecular cloud in ^{12}CO and ^{13}CO covering the entire extent of the cloud. We analyze global structure, mass, and kinematics of the cloud, and discuss its evolutionary status.

II. OBSERVATIONS

A 2.4 square degree region centered on the position of the S287 HII region ($l = 218°.1$, $b = -0°.4$) was mapped in the transition of ^{12}CO $J = 1-0$ with the QUARRY fifteen beam array receiver on FCRAO 14 m telescope between May and June 1992. A 0.8 square degree was also mapped in the transition of ^{13}CO $J = 1-0$, which encompasses most of ^{12}CO emission. ^{12}CO map consists of $\sim$ 12,400 spectra, and ^{13}CO map consists of $\sim$ 3,800 spectra. Two filterbanks with thirty-two channels each having frequency resolutions of 250 KHz and 1 MHz were used for each beam. A velocity coverage of 21 km s^{-1} and resolution of 0.65 km s^{-1} is therefore provided with the 250 KHz filterbank at the frequency of the ^{12}CO $J = 1-0$ line. The 1 MHz filterbank provided a velocity coverage of 85 km s^{-1} with a resolution of 2.6 km s^{-1} , and was used to check if emission at other velocities was detectable toward the cloud.

All observations were made by repeatedly switching to one position at $l = 216°.9$, and $b = -0°.5$ confirmed to have no CO emission. Each reference observation was shared with observations at 4 to 6 map positions depending on the sky stability. Calibration was accomplished by frequently observing an ambient temperature load. All antenna temperatures quoted are corrected for atmospheric extinction and for the forward spillover and scattering losses of the antenna and radome ($\eta_{fss} = 0.7$ at 110 to 115 GHz), and are therefore on the T_R^* temperature scale defined by Kutner and Ulich (1981). The average rms noise of the data was 0.4 K in ^{12}CO, and 0.2 K in ^{13}CO.

III. RESULTS

(a) Cloud Morphology and Velocity Structure

The ^{12}CO integrated intensity map of S287 molecular cloud is presented in Figure 1 superposed on grey-scaled map of IRAS flux at 100 μm. The cloud has an extent of 1.5 degree in Galactic longitude, and tilted about 30 degrees with respect to the Galactic plane. The morphology of the molecular gas is very elongated and also filamentary. There are several hot molecular clumps, which are matching with regions with strong IRAS flux. Outside the main emission region, several small patches of molecular gas are dispersed. However, the two patches of clouds centered at $l = 217°40', b = 0°10'$ and $l = 218°, b = 0°10'$ are not likely associated with the main cloud as their velocity range (+21 to +23 km s^{-1}) is significantly different from that of main cloud, and has no sign of gas connection (see below). The positions marked with A to E are representing outflows listed in Iwata *et al.* (1989)'s unpublished paper referred by Fukui (1989). These are all matching with the IRAS point sources.

Maps of the cloud at individual velocities are shown in Figure 2. One spectrometer channel was presented in each map (0.65 km s^{-1} per channel) and the velocity range covered is +21 to +31 km s^{-1}. These maps shows very intriguing velocity field. The velocity of main cloud is starting from $\sim$ +23 km s^{-1} and is extended up to $\sim$ +31 km s^{-1}. Channel map shows that the main cloud has been severely disturbed. The cloud is comprised of three major components; southern, northern, and middle components. Southern component is located at $l = 218°12', b = -0°40'$ in Figure 1, and northern component is starting at $l = 217°40', b = -0°15'$ and extended up to $l = 217°00', b = 0°10'$ in diagonal direction. The rest part of the main cloud is middle component. The length of each cloud is about 10 to 15 pc assuming a distance of 2.2 kpc (Lee *et al.* 1994). In Figure 2, the middle component and southern component appear at the velocity of +24 km s^{-1}, and are being dispersed at the velocity of +25.4 km s^{-1}. The middle component is growing into the diagonal direction as the velocity increases, while the southern component seems to be relatively stable except small filaments which appear at the velocity of $\sim$ +25 km s^{-1}. The tail of the northern filamentary component centered on $l = 217°20', b = -0°05'$ is growing as the velocity is increased, and finally it is being detached from the main component. The more spreaded filamentary structure is also present in the middle component, and is being spreaded to the same direction as that of northern component. The CO linewidths of the cloud are very broad ($\Delta V \simeq 6$ km s^{-1}) and emission strength is very hot (15 K), which is within the range of typical

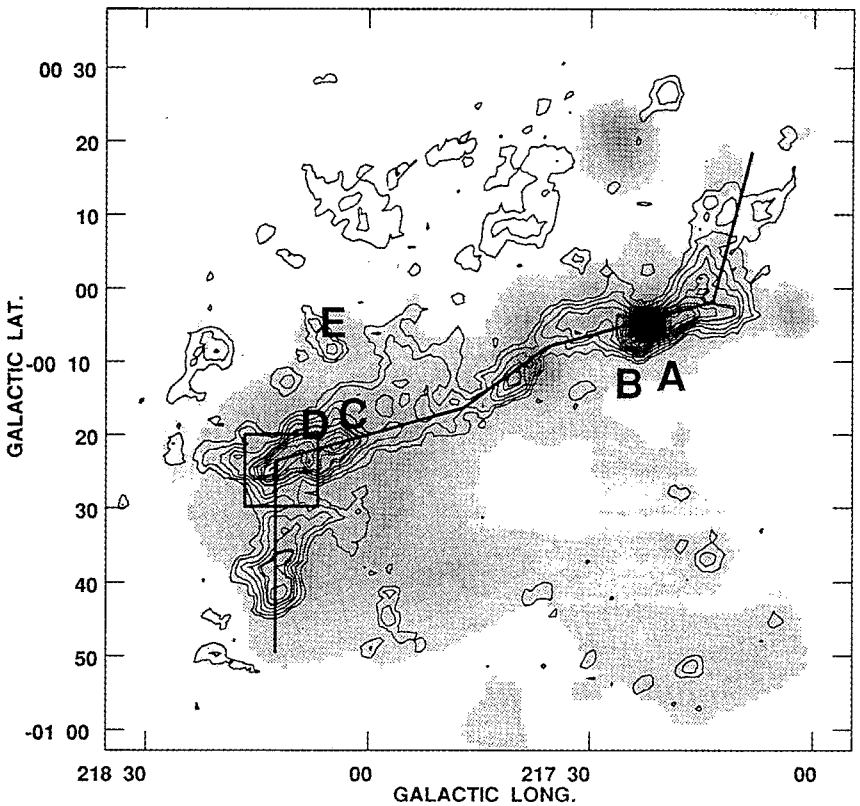

Fig. 1. The ^{12}CO integrated intensity contour map of S287 molecular cloud superposed on the IRAS flux grey-scaled map at 100 μm . The lowest contour level and the increment between the levels are 2.5 K km s^{-1}. A to E are representing the positions of outflows which are reported by Fukui (1989). The grey scale ranges from 30 to 300 MJy/sr. The highest flux arise around the location marked with A and B with a value of 450 MJy/sr. Solid line represents the spatial-velocity cut (Figure 3), and box represents the region of composite spectra shown in Figure 6.

GMC's parameters.

Figure 3 is the spatial-velocity cut along the three main components of the cloud. The direction of the cut is shown as a solid line in Figure 1. The 'distance' axis is in the unit of acrminute along the cut direction, and the 'velocity' axis is in the unit of km s^{-1}, covering the whole range of 250 KHz filterbanks. The velocity field is striking: it shows several arcs and the broad linewidths. The mean velocity of the cloud is $\sim +26.5$ km s^{-1} and the velocity range is from +22 to +32 km s^{-1}The embedded outflows (Fukui 1989) are represented as capital alphabet letters, A to D (E is not included in Figure 3). Outflows A and B show typical spatial-velocity map, though the cut direction is not exactly along their axes. The combined momentum estimate was few hundred $M_\odot$ km s^{-1}, and the kinetic energy generated was estimated to be $\sim 10^{44-45}$ erg (Iwata *et al.* 1989).

Small italicized-alphabet a, b, and c are regions which can be described as remarkable arcs and/or shell-like structure. The arc-shaped structure can be seen in the channel maps as well as in the position-velocity map, which implies that the cloud is being perturbed severely by external driving sources. One major source is, of course, the HII region S287 residing at $l = 218°.1$, $b = -0°.4$. This is the only prominent origin which makes very powerful driving source. The driving power of the HII region can be partially imagined from Figure 4, which is ^{12}CO intensity map of blue and red-shifted components of the cloud. These are not related to outflow wings, but arbitrarily divided. The red-shifted component of the cloud is presented in grey-scaled map ($V_{LSR} = +23$ to $+25$ km s^{-1}), and the blue-shifted component is presented in contours ($V_{LSR} = +29$ to $+32$ km s^{-1}). The velocity range shown in Figure 4 is very broad and describes that cloud is being disrupted severely. The solid circle is the approximate boundary of the HII region S287. The thinner solid lines marked with D1, and D2 are the cut directions (from lower right to upper left) to generate spatial-velocity maps.

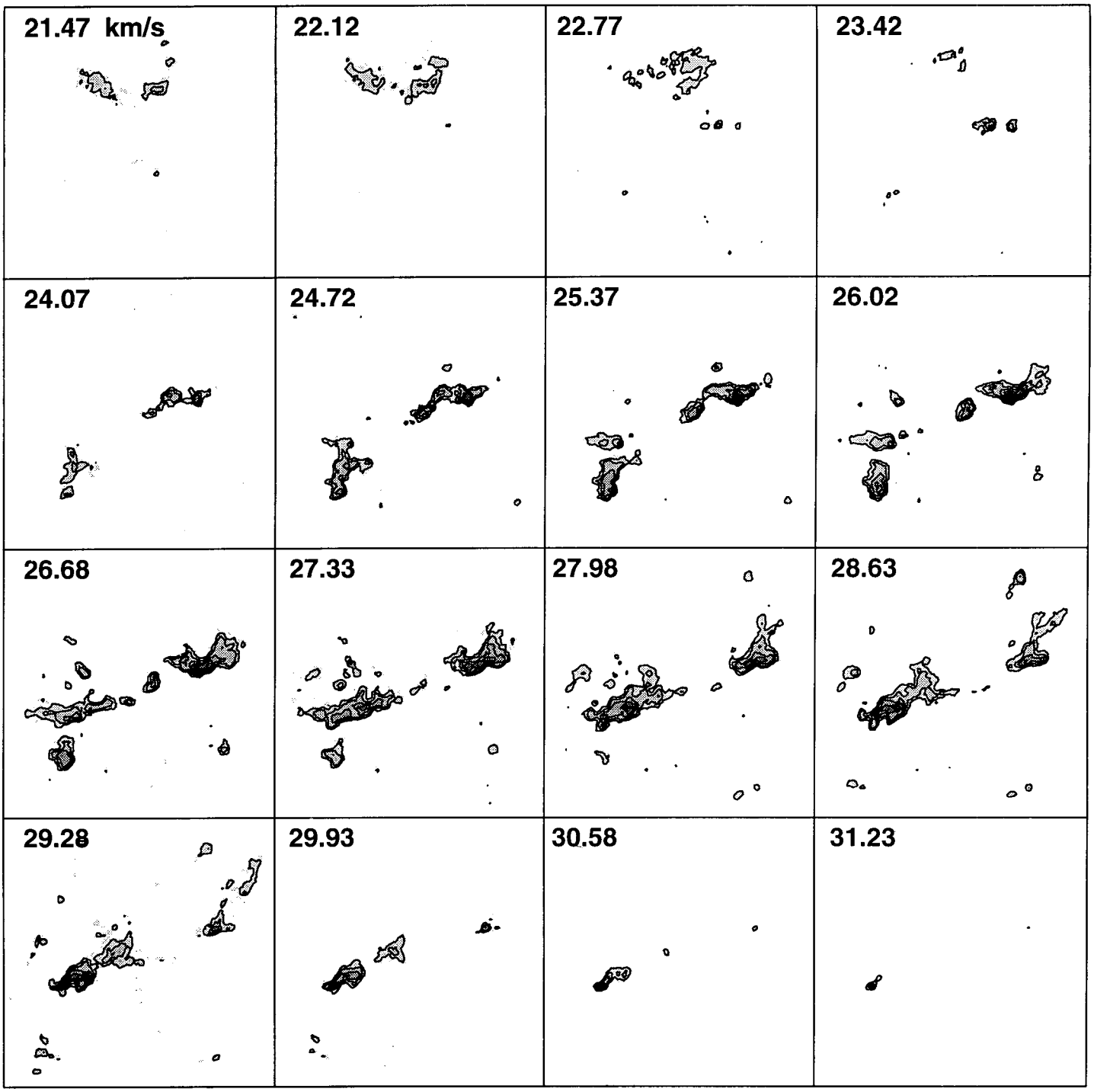

Fig. 2. The ^{12}CO velocity maps of S287 molecular cloud. Each map has V_{LSR} range of 0.65 km s^{-1}, which is corresponding to one channel of 250 KHz spectrometer. The contour levels are 1.5, 3, 5, and 8K. The centered velocity of each map is marked at the upper-right corner.

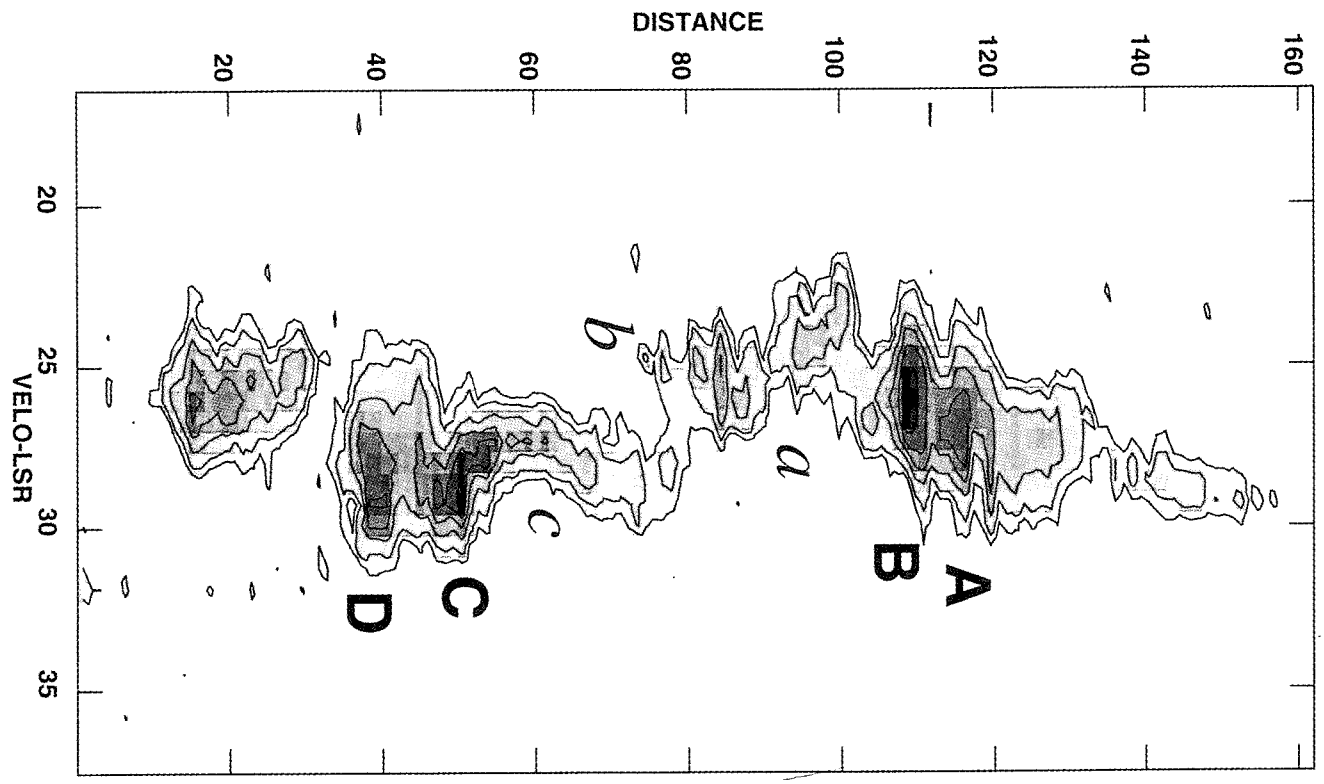

Fig. 3.. A ^{12}CO position-velocity map for the diagonal cut across the main body of the cloud. The Distance axis is in the unit of pixel size, 50″, thus the whole length of the cut is ~ 2.5 degrees. The cut line is not necessarily straight, rather along the strong emission region from the lower left to the upper right, which is marked with a solid line in Figure 1, including outflows A to D. The grey scale ranges from 0.7 to 12 K. The lowest contour level is 1 K, and the increment between the levels is 2 K. The italicized alphabet a to c are representing prominent arcs(see text).

Figure 5 represents a spatial-velocity map of D1 cut marked in Figure 4. The D1 cut starts from the filament of the southern component of the cloud, including the boundary of HII region, and through the lower left filamentary element of middle component. This spatial-velocity map show the most striking feature. Velocity widths of two filamentary elements are very broad comparing with other part of the cloud. Southern filamentary component marked as 'S' has a huge velocity range from +21 km s^{-1} to +28 km s^{-1}, which is obvious sign of being expanded, likely driven by the HII region. Middle filamentary also shows significant velocity gradient with a velocity-loop. Intriguingly, the position of this velocity-loop marked as 'Loop M' is the just at the boundary of the HII region (Figure 4). 'Loop M' represents a direct example of interaction of ambient molecular cloud and HII region. One hundred and twenty one composite spectra (Figure 6) centered on the boundary of HII region ($l = 218°.15, b = -0°.28$) represent the interacting phenomena more clearly: From the center of Figure 6 the lines are dividing into two components, generating filamentary (wing) structure as described above. This feature is more obvious in the lower part of the region. The spectra shown in Figure 6 are all non-gaussian profiles, which is a clear clue that the cloud is being perturbed.

The D2 cut (Figure 7) is starting from the upper part of the middle cloud component and extended up to the small patch of cloud, where Iwata *et al.* (1989) identified one outflow. However, we were not able to confirm its wings therein, probably because of lower sensitivity of our data (rms noise of ^{12}CO is 0.4 K). The filamentary element in Figure 7 has a clear velocity gradient, 0.3 km s^{-1}/pc, which is a clear evidence for external perturbation.

Overall, the velocity structure of the cloud is disturbed by external and internal driving sources: it appears that the cloud may have been severely disrupted and the molecular gas is being distorted by series of strong stellar wind or shock. Further discussion of the kinematics of the cloud will be presented in detail in later section.

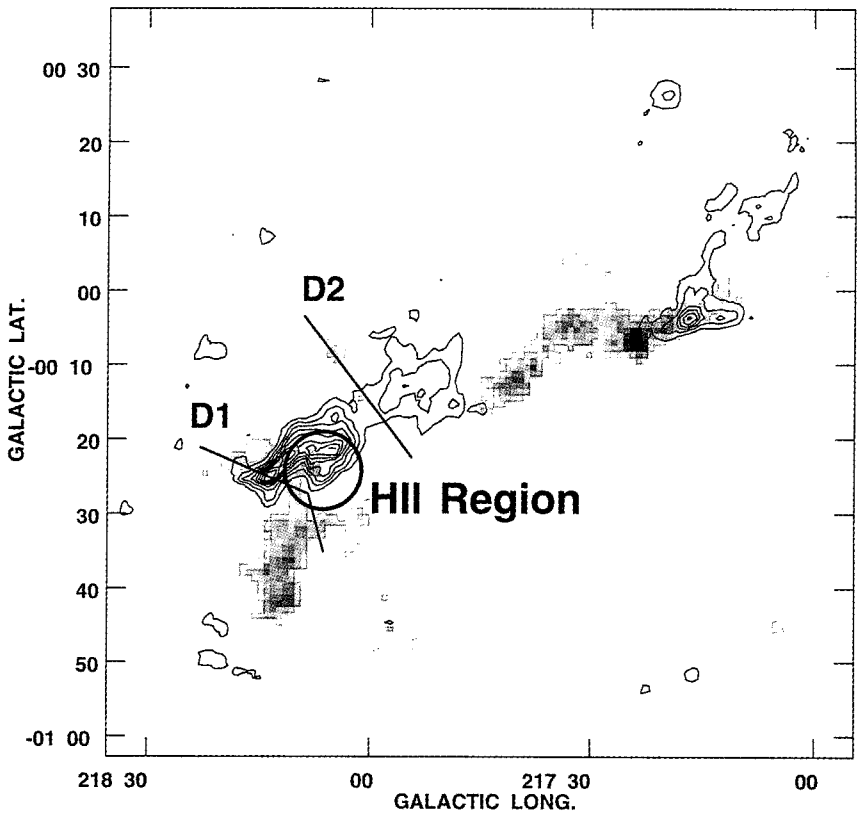

Fig. 4. The ^{12}CO integrated intensity map for blue-shifted and red-shifted components. The red-shifted component is for the velocity range of +22 to +25 km s^{-1} and represented in grey-scaled map, and grey scale ranges from 2 to 25 K km s^{-1} . The blue-shifted component (+28 to +33 km s^{-1}) is presented in contours. The lowest contour is 0.8 K and the contour increment between the levels is 1 K. The solid circle represents the position of HII region S287.

(b) Mass Estimate

Three different techniques for estimating the mass of S287 molecular cloud are described in this section. A technique that has been widely used to estimate a cloud mass is the LTE method. More detailed discussion of this technique and assumption inherent in its use can be found in many papers (Lee 1992 and 1994; Dickman 1978). With the correlation of visual extinction obtained by Lee *et al.* (1992) and ^{13}CO column density, the LTE mass for S287 molecular cloud is estimated to be 1.3×10^4 $M_\odot$.

If a molecular cloud is virialized (gravitationally bound, and has had enough time to be dynamically relaxed), then the partition of energy will be governed by the virial theorem. In that case, the virial mass is given by

$$M_{VIR} = \frac{3\alpha\sigma_{tot}^2}{2G} D, \quad (1)$$

where D is the cloud diameter and σ_{tot} is velocity dispersion of the cloud, which represents all forms of kinetic motion within the cloud. The constant α is order of unity (α = 1.6 was adopted assuming a uniform density distribution; see Lee *et al.* 1991) and depends on the shape and density distribution of the cloud. Since clouds are irregularly shaped, it is not straightforward to define a cloud size. The morphology of S287 molecular cloud is very elongated and filamentary. It has about 30 pc long and 5 to 10 pc wide along the diagonal direction, thus we adopt the size of the cloud as the mean of two axes, 20 pc. However, the determination of size is not very significant for determining the mass of the cloud. This fact will be described in Discussion section. The velocity dispersion of the cloud is estimated to be 2.43 km s^{-1}, and thus the estimated virial mass is 7.2×10^4 $M_\odot$.

Another mass estimate can be obtained by using the empirical relationship between the CO integrated intensity and molecular hydrogen column density, or equivalently, the relationship between CO luminosity and mass. The

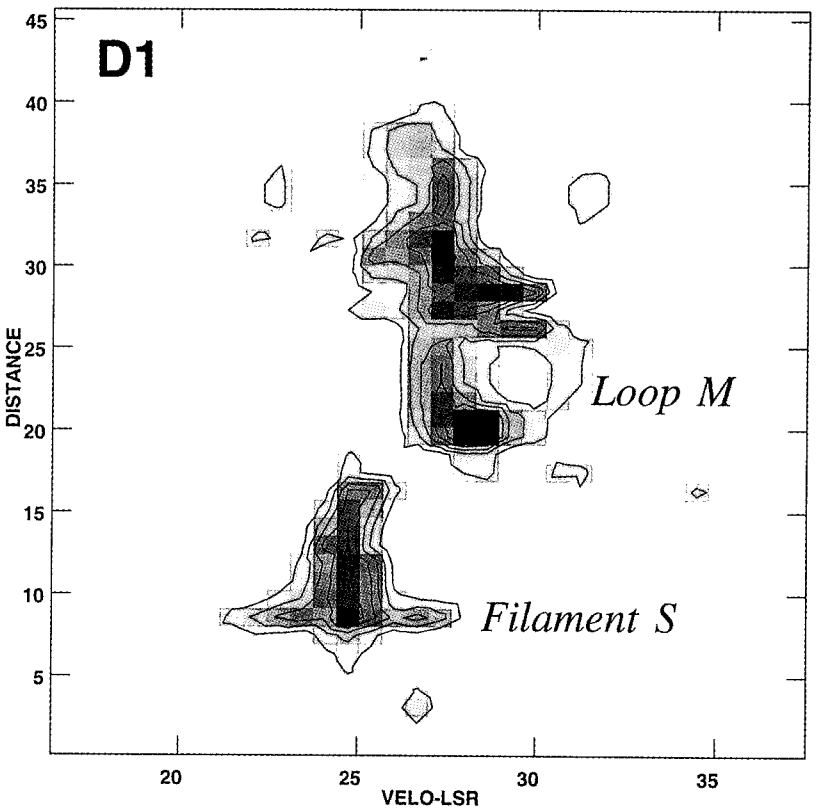

Fig. 5. The D1 position-velocity map of the diagonal cut starting from the lower right, through part of the HII region, and up to left upper direction. The grey scale ranges from 0.5 to 5.5 K. The lowest contour level and the increment between the levels are 0.8 K, respectively. The obvious filament and loop are marked as S and M, respectively (see text).

^{12}CO luminosity of S287 is 5.62×10^3 K km s^{-1}. Thus, if we use the most recent estimate of the conversion factor established through γ-ray analysis, 2.3×10^{20} cm^{-2} (K km s^{-1})$^{-1}$ (Bloeman 1989), we obtain a mass of 2.8×10^4 $M_\odot$.

(c) Cores and Density

There must be several dense cores in S287 molecular cloud. In this paper we did not include CS observations toward dense cores. However, from the ^{13}CO peak temperature map shown in Figure 8 the distribution of hot spots, which are the candidates of dense cores, can be seen more easily than in ^{12}CO integrated intensity map (Figure 1). The weak grey colored background boxes present the mapped region with ^{13}CO, and the lowest contour level and contour increment are 1 K, respectively. We are planning to study these cores in other paper.

Taking the total mass of S287 molecular cloud as 1.3×10^4 solar masses (see below), we can estimate the volume density of the cloud. The length was estimated to $\sim$ 30 pc and the width was 5 pc. The third axis of the cloud is unknown, however, it should not be much larger or smaller than other axes. Thus, we take the length of third axis as the geometric mean of other two axes, 12 pc. Thus, the volume density was estimated to be order of hundred per cubic centimeter, which is a typical value of GMCs (Goldsmith 1988).

IV. DISCUSSION

(a) Mass Discrepancy

We have estimated cloud mass in three different methods: the LTE estimate, 1.3×10^4 $M_\odot$, is the smallest, and

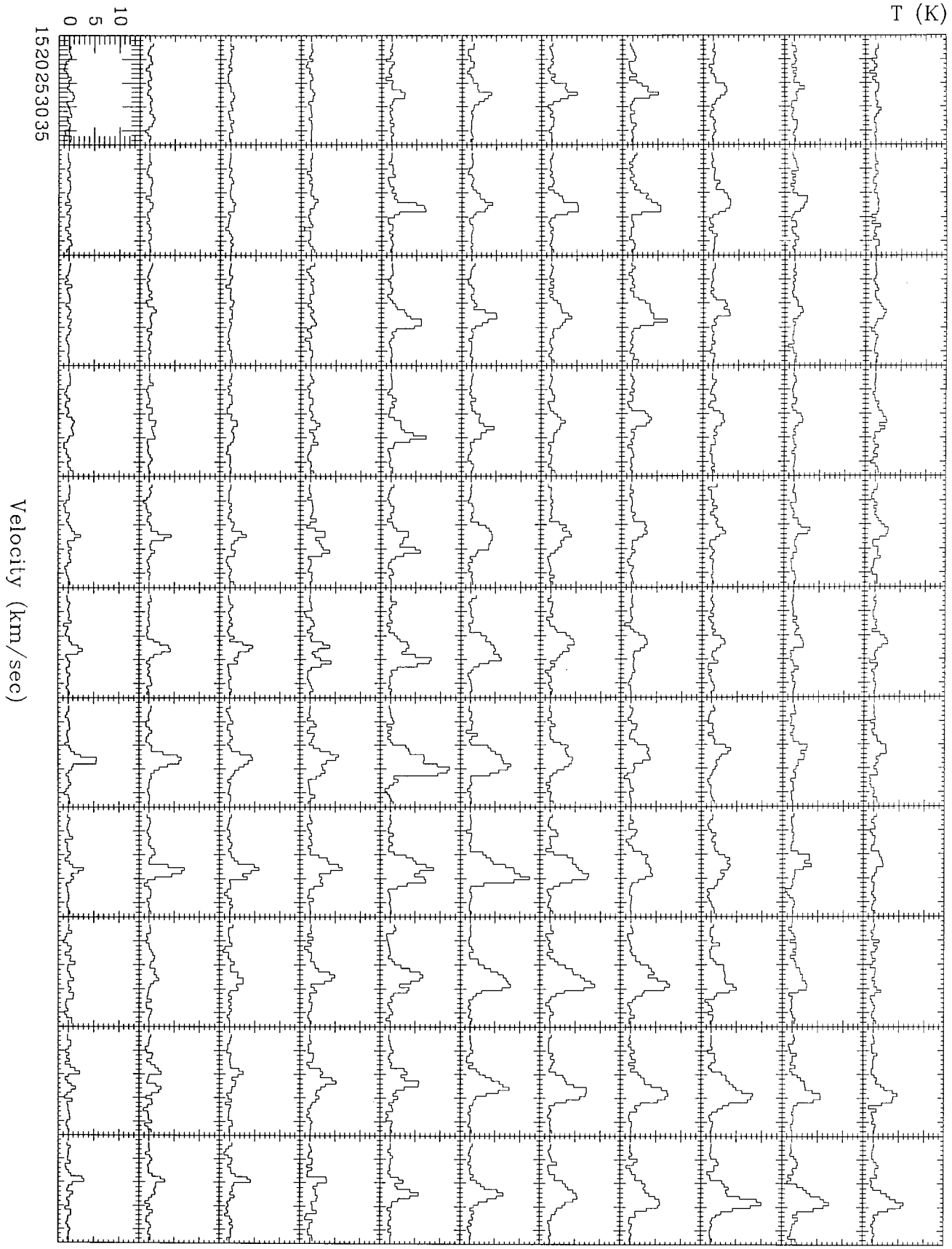

Fig. 6. The ^{12}CO composite spectra centered on $l = 218°.3, b = 0°.4$ (marked as a box in Figure 1) beside the HII region.

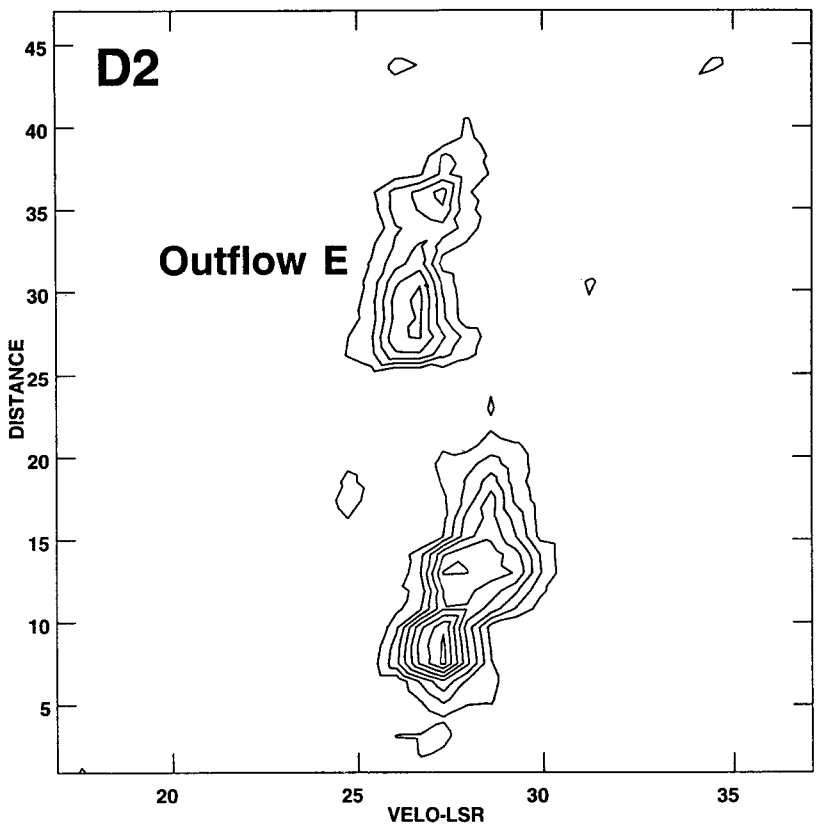

Fig. 7. The position-velocity map of the diagonal cut D2 from the lower right to left upper direction, including a small outflow E. The lowest contour level and the increment between the levels are 0.8 K, respectively.

the virial estimate, 7.2×10^4 $M_\odot$, is the largest one.

Many parameters, such as velocity dispersion, size and density enters the virial mass estimate. The size is the most poorly determined parameter as the cloud morphology is very elongated, and filamentary. Lee (1992, 1994) have fully discussed on the size determination, and argued that the size definition depends on the sensitivity of CO observations. To avoid this problem, he compared various definitions of cloud size, and found that the largest difference entered is $\sim$ 30%. Thus, the size definition will affect the virial estimate within 30%. The different density distribution model will affect at most 20% of virial mass estimate (Lee 1992, 1994). Thus, these two parameters will not affect virial estimate significantly if a cloud is virialized.

We have obtained two velocity dispersions of the cloud to decompose cloud's internal motion and turbulence motion. While the estimated internal velocity dispersion of the cloud is 1.04 km s^{-1}, the centroid velocity dispersion of the cloud is 2.2 km s^{-1}, a factor of two larger than the internal velocity dispersion. The centroid velocity dispersion is representing the bulk motions of the gas within the cloud (Lee *et al.* 1990). Thus, if a cloud has a systematic motion, such as rotation or expansion/collapse, or internal/external disturbance, its centroid velocity dispersion should be much larger than its internal velocity dispersion. This is a good measure of cloud's kinematics. On the other hand, most of the GMCs are reported to be virialized even though they are associated with star forming activities with a few exceptions (Scoville *et al.* 1987). Their centroid velocity dispersions are fairly comparable with their internal velocity dispersions statistically. This fact seems to be more likely for much larger clouds with $> 10^6$ $M_\odot$.

The conversion factor in the CO luminosity-mass relation has been established through many ways including γ-ray analysis. We have used a recent estimate of the conversion factor of 2.3×10^{20} cm^{-2} (K km $s^{-1})^{-1}$ (Bloemen 1989), and obtained a mass of 2.8×10^4 $M_\odot$. However, one may still have reasons to be concerned about this estimate. The existence of a general relation between mass and CO luminosity may be the result of most clouds being in virial equilibrium (Lee 1992, 1994). If S287 molecular cloud is not in virial equilibrium, its mass could be

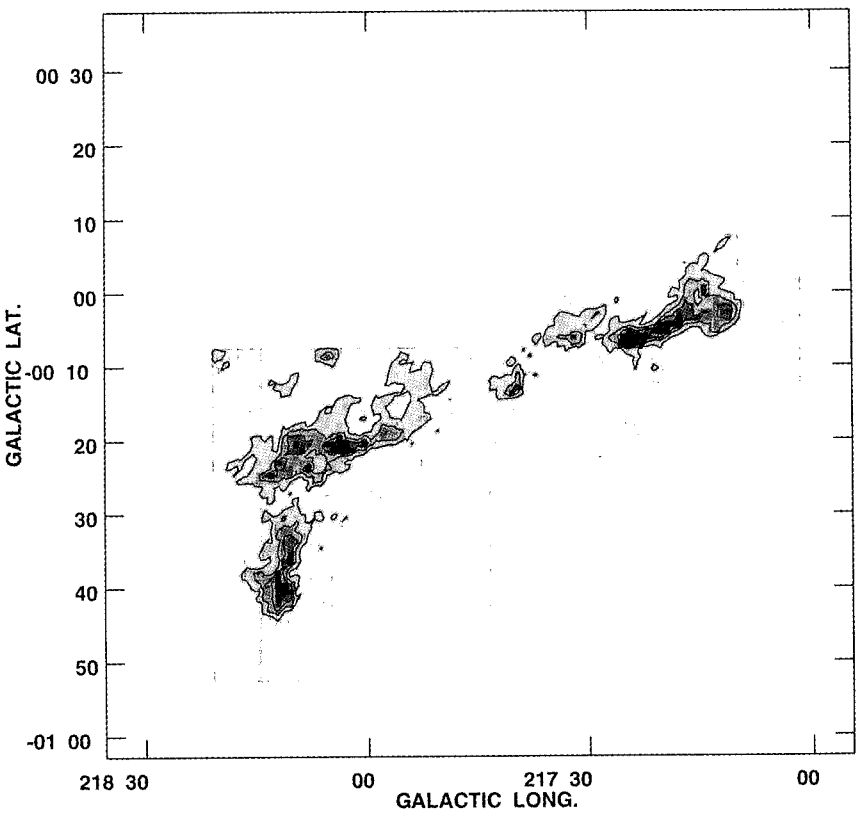

Fig. 8. ^{13}CO peak temperature map. The range of the grey scale is from 0 to 5 K. The lowest contour level and the increment of between the levels are 1 K.

overestimated by this technique.

It has been long debate that LTE mass estimate might significantly miss the mass outside the cloud boundary, and that it is based on several critical assumptions. A critical assumption is the equal excitation temperature along the line of sight, which affect the determination of ^{13}CO column density. However, there are many studies that NLTE model prediction of ^{13}CO column density have been made, and that the method recovered the original model column density for the volume density higher than a few thousand per cubic centimeter (Lee 1992 and reference therein).

Most significant sources of error in LTE technique arise from adopting the ^{13}CO abundance. The popular method to obtain the ^{13}CO abundance was estimating the visual extinctions and applying a universal extinction to gas column density ratio. While a correlation between proton column density and extinction was empirically established by Bohlin, Savage, and Drake (1978), it was only established for $A_V < 2$ magnitudes. Thus, it is necessary to extrapolate their correlation in order to apply it to molecular clouds, implicitly assuming that the grain properties are the same as in lower density regions. Fortunately, we have a well-established correlationship between the visual extinction and ^{13}CO abundance for the core region of G216-2.5 (Lee, Snell, Dickamn 1991), which is considered to be a remnant cloud of a progenitor star-forming complex, including S287 molecular cloud (Lee *et al.* 1994). Since the visual extinction for only small portion of G216-2.5 is greater than 4 magnitudes, our extinction measurements should be generally applicable. Moreover, the mass outside of the cloud boundary can be compensated if we include the intercept of this correlation as discussed by Lee (1992 and 1994).

Thus, we believe that the LTE mass estimate for S287 molecular cloud is reliable.

(b) Kinematics and Evolutionary Status

S287 molecular cloud has a very intriguing velocity structure. It shows more severely disturbed morphology than typical GMCs. There are many star forming regions, outflows, and several arcs in position-velocity map as well as in

^{12}CO intensity map. Accordingly, its kinematics can be attributed to external forces, as is suggested, perturbation. A couple of candidates for perturbation sources can be considered; an old HII region, or combination of several HII regions could be one possibility. Old supernova remnant and/or combination of them is the second possibility. A single stellar wind can produce a huge amount of energy up to $\sim 10^{46-47}$ erg, and SNR shock could have produced more energy. As the total kinetic energy of the cloud is $\sim 10^{48}$ erg, and if a fraction of it kinetic energy is replenished by perturbation, those scenarios seem to be quite plausible. As the predicted supernova rate is one in every 20 to 50 years in the Galaxy (Sramek *et al.* 1992), those scenario may be possible.

Those peculiar phenomena drive a fundamental question; what would be the evolutionary status of S287 molecular cloud ? At least, we have four clues supporting . First, the velocity dispersion of S287 molecular cloud is relatively large, which causes much larger virial mass estimate. Thus, the discrepancy between LTE and virial masses might be explained if the cloud is being severely perturbed. Second, there is some enhancement in continuum survey at 408 MHz toward the S287 and G216-2.5 (Haslam *et al.* 1981). Though its resolution (FWHM is a half degree) was coarse, the enhancement is fairly obvious. This fact suggests that it has some sign of ionization, or somewhat shocked by old SNR or strong stellar winds. Third, the filamentary structures have been evidence for being swept-up by violent stellar wind: the filamentary structure without young stars was found on the edge of Orion cloud (Bally *et al.* 1987), which is one of the best example that ambient molecular gas was fluctuated. Lac OB1, which is one of the oldest OB associations in solar neighborhood with an age of $\sim 2 \times 10^7$ years (Blaaw 1964), has also remnant of molecular gas. Its structure is very fragmentary and the most of gas are almost dispersed. Its whole range of remnant is $\sim$ 10 pc, smaller than S287 molecular cloud. Fourth, a recent study shows a similar example to S287 and G216-2.5 on the arc region of Gem OB1 (Carpenter 1994); up to 32 square degree centered on Gem OB1 molecular cloud complex was mapped in ^{12}CO and ^{13}CO resonance transition line with high resolution sampling rate as in the case of S287 and G216-2.5. The morphology of the molecular clouds associated with Gem OB1 is dominated by filaments and arcs of molecular material, presumably formed by expanding HII regions and stellar winds from young stars within the cloud. One of the molecular clouds at $\alpha = 05^h57^m$, $\delta = +20°$ within the Gem OB1 complex has properties very similar to those of G216-2.5. However, this cloud is clearly part of a much larger arc of molecular gas that encircles the S252/S247 star forming regions. S287 HII region and its associated molecular cloud are similar to Gem OB1 complex in this aspect, though the scale of active star formation is smaller than that of Gem OB1 complex.

A warmer GMC, S287, is located $\sim$ 100 pc from G216-2.5, and is probably physically related to G216-2.5 as discussed earlier. This clue and the evolutionary status of these two clouds has been discussed in more detail by Lee *et al.* (1994). They favored an evolutionary state that places it between episodes of massive star formation based on several reasons. The most intriguing reason they are concerned is that one can use the very striking similarities between G216-2.5 and Gem OB1-c to argue that both clouds are in similar evolutionary states, and for Gem OB1-c the evidence that it is part of a shell produced by the past star formation activity is much more convincing. Thus, we believe that S287 and G216-2.5 are remnant clouds from an older star formation event and that S287 molecular cloud may be starting second generation of star forming activities.

V. Summary

We have obtained high-resolution maps toward a molecular cloud associated with an HII region S287 in the transitions of ^{12}CO and ^{13}CO $J = 1 - 0$. We summarize the results of present study as follows:

- We have discussed three different mass estimate techniques, and obtained a large range of mass, 1.3×10^4 $M_\odot$ to 7.2×10^4 $M_\odot$, depending on the techniques. The factor of 6 discrepancy between the virial and LTE mass estimate is much larger than expected based on the uncertainties in two methods. The large virial mass and the very disturbed morphology may reflect the fact that is not gravitationally bound system, as in the case of nearby cloud G216-2.5. In fact, the cloud has much larger centroid velocity dispersion, an indicator of perturbation.
- The cloud shows a very disturbed feature: velocity field of the cloud is very complicated, and shows several arcs. The southern part of cloud is being disrupted mainly by the residing HII region S287 and external sources. In addition to HII region, there are several bipolar outflows, which also disturbing the molecular gas significantly. The several arcs and the filamentary features are possibly driven by external strong stellar winds. These external

sources may be driving the second generation of star-forming activities on the edges of the clouds.

ACKNOWLEDGEMENTS

This research has been supported by Korea Astronomy Observatory's Basic Research Fund Program.

REFERENCES

Bally, J., Langer, W.D., Stark, A.A., and Wilson, R.W. 1987, *ApJ*,312, L45.
Blaww, A., 1964, *ARAA*, 2, 213.
Blitz, L., 1991, in *The Physics of Star Formation and Early Stellar Evolution*, eds. C. H. Lada and N. D. Kylafis. (Dordrecht: Kluwer Academic Publishers), p. 1.
Bloemen, J. B. G. M. 1989, *ARAA*, 27, 469.
Bohlin, R. C., Savage, B. D., and Drake, J. F. 1978, *ApJ*, 224, 132.
Carpenter, J. M., 1994, Ph. D. Dissertation, University of Massachusetts.
Dickman, R. L. 1978, *AJ*, 83, 363.
Fukui, Y. 1989, in *ESO Workshop No. 33; Low Mass Star Formation and Pre-main Sequence Objects*, ed. B. Reipurth, p. 95.
Goldsmith, P. F. 1988, in *Molecular Clouds in the Milky Way and External Galaxies*, eds. R. L. Dickman, R. L. Snell, and J. S. Young (Dordrecht: Reidel), p. 1.
Haslam C.G.T. Salter, C.J., Stoffel, H., and Wilson, W.E. 1981, *AAS*, 47, 1
Iwata, T. *et al.* 1989, unpublished paper.
Kutner, M. C., and Ulich, B. L. 1981, *ApJ*, 250, 341.
Lee, Y., Snell, R. L., and Dickman, R. L. 1990, *ApJ*, 355, 536.
Lee, Y., Snell, R.L., Dickman, R.L. 1994, *ApJ*, 432, 167.
Lee, Y. 1992, Ph. D. Dissertation, University of Massachusetts.
Lee, Y. 1994, in press, Publication of Korean Astronomical Society.
Lynds, B.T. 1962, *ApJS*, 7, 1.
Lynds, B.T. 1965, *ApJS*, 12, 163.
Neckel, T., Staude, H. J., Meisenheimer, K., Chini, R., and Gusten, R. 1989, *A.A.*, 210, 378.
Scoville, N. Z., Yun, M. S., Clemens, D. P., Sanders, D. B., and Waller, W. H. 1987, *ApJS*, 63, 821.
Scoville, N. Z., and Sanders, D. B. 1987, in *Interstellar Processes*, eds. D. J. Hollenbach and H. A. Thronson, Jr., p. 21.
Scoville, N. Z., and Sanders, D. B. 1987, in *Interstellar Processes*, eds. D. J. Hollenbach and H. A. Thronson, Jr., p. 21.
Sramek, R.A., Cowan, J.J., Roberts, D.A., Goss, W.M., and Ekers, R.D. 1992, *AJ* 104, 704.